Journal of Engineering Mathematics, Vol. 3, No. 2, April 1969
Wolters-Noordhoff Publishing – Groningen
Printed in the Netherlands

Dissipative Difference Schemes for Shallow Water Equations

A. C. VLIEGENTHART

Delft University of Technology, Dept. of Mathematics, Delft, the Netherlands

(Received December 11, 1968)

SUMMARY

Three dissipative finite-difference schemes are discussed for the numerical calculation of discontinuous shallow water flow. The shallow water equations have been derived on assumptions which are not acceptable in the case of discontinuous flow. However, they may give satisfactory results if only weak jumps are present.

It will be shown that a coarse network may affect the velocity of propagation of the computed bore.

1. Introduction

The nonlinear shallow water equations derived by Stoker [1] are frequently used for continuous solutions to problems concerning shallow fluid flow.

In this paper, we discuss three dissipative finite-difference schemes for approximating discontinuous shallow fluid flow governed by the shallow water equations.

The schemes are tested for stability, numerical damping and phase shift. The Courant-Friedrichs-Lewy stability condition appears, though the schemes are dissipative if this condition is slightly strengthened.

In [2] Leendertse had to deal with numerical damping as a falsification of the solutions of his calculations of long-period water waves. This damping is necessary if we are to obtain a stable solution in our calculations.

As in [2] the numerical phase shift influences the solution, but is minimized by a refinement of the superimposed grid.

By a nonlinear combination of the shallow water equations, we obtain a second system of equations. The two systems are equivalent in the case of smooth solutions, but yield different solutions if a discontinuity occurs in the flow. We shall arrive at a system which is physically acceptable for our computations.

The results obtained from the jump conditions at the discontinuity in the flow are favourably compared with the numerical solutions. Results from laboratory experiments carried out by Cavaillé [3] give an indication of the usefulness of the shallow water equations as a computational model for discontinuous shallow fluid flow.

2. Preliminary Considerations

We consider the initial-value problem for the class of equations of the form

$$u_t + f_x = 0\,, \qquad 0 \leqq t \leqq T, \text{ and } u(x,0) = \varphi(x)\,, \tag{2.1}$$

where $u(x, t)$ is a p-component vector and $f(u)$ is a known vector-valued function of u.

Suppose that equation (2.1) can be transformed into

$$u_t + A(u)u_x = 0\,, \tag{2.2}$$

where $A(u)$ denotes the Jacobian matrix of f with respect to u. Let the quasi-linear system (2.2) be hyperbolic, i.e., the matrix A has p real and different eigenvalues a_ν for all values of the argument u.

We approximate the system (2.2) by means of explicit difference schemes of the form

$$v(x, t+\Delta t) = S_{\Delta x} v(x, t) , \tag{2.3}$$

in which Δt represents the time increment and $S_{\Delta x}$ a finite sum of translation operators with matrix coefficients,

$$S_{\Delta x} = \sum_{(j)} C_j T^j .$$

The operator T denotes translations by amounts $\Delta x = \Delta t/\lambda$ in the x-direction, λ being constant independent of Δx and Δt, $T^j v(x, t) = v(x+j\Delta x, t)$.

Definition. *The differential equations* (2.2) *are approximated with m-th order accuracy by means of the difference scheme* (2.3) *if for all sufficiently smooth, genuine solutions* $u(x, t)$ *of* (2.2),

$$\|u(x, t+\Delta t) - S_{\Delta x} u(x, t)\| = O(\Delta t^{m+1}) \quad as \quad \Delta t \to 0$$

holds uniformly in t.

The norm appearing in this definition denotes the L_2 norm. We assume that the calculations will be performed from $t=0$ to $t=T$. For this time range we require the difference scheme (2.3) to be stable, ignoring the influence of the boundary conditions.

Definition. *The difference scheme* (2.3) *is (Lax-Richtmyer) stable if for some* $\sigma > 0$, *a constant* M *exists such that*

$$\|S^n_{\Delta x}\| \leqq M$$

for all n, Δt *satisfying* $0 < \Delta t < \sigma$, *and* $0 \leqq n\Delta t \leqq T$.

In the nonlinear case we consider the first variation of the operator $S_{\Delta x}$, and then replacing the variable coefficients by their value at some given point, we obtain the "localized" operator. For stability of $S_{\Delta x}$ in the nonlinear case we require the associated "localized" operator to be stable at every point. Suppose that $u(x, 0)$ has period q in x, then the local amplification matrix G of $S_{\Delta x}$ will be defined by

$$G(x, \Delta t, \xi) = \sum_{(j)} C_j e^{ij\xi} ,$$

where $\xi = k\Delta x$; k is dual to x in the Fourier transform and ranges over the values $2\pi r/q$, r being any integer.

According to Richtmyer and Morton [4] the aforementioned stability condition involves the uniform boundedness of the matrices G^n and yields the von Neumann necessary condition for the eigenvalues g_ν of G:

$$|g_\nu(x, \Delta t, \xi)| \leqq 1 + O(\Delta t) , \qquad 0 < \Delta t < \sigma, \ \nu = 1, 2, \ldots, p . \tag{2.4}$$

In [4] the following is proved:

Theorem. *If the amplification matrix* G *has a complete set of linearly independent eigenvectors, then condition* (2.4) *is sufficient as well as necessary for stability if a constant* τ *exists such that* $\Delta \geqq \tau > 0$, *where* Δ^2 *is the Gram determinant of the normalized eigenvectors.*

In the next sections we shall discuss dissipative difference schemes.

Definition. *The difference scheme* (2.3) *is dissipative of order* $2r$, *where* r *is a positive integer, if there is a positive constant* δ, *such that*

$$|g_\nu(x, \Delta t, \xi)| \leqq 1 - \delta |\xi|^{2r}, \qquad \nu = 1, 2, \ldots, p$$

for all x *and all* ξ *and* Δt *satisfying* $|\xi| \leqq \pi$, *and* $\Delta t < \sigma$, *where* σ *is some positive constant number.*

3. Numerical Damping and Phase Shift

The definition of the amplification matrix G in the preceding section presupposes a component $\hat{u}(k)e^{ikx}$ of the Fourier series for $u(x, 0)$. This component changes for the genuine solution $u(x, t)$ of system (2.2) with constant matrix A into

$$\hat{u}(k)e^{i(kx-lt)}, \tag{3.1}$$

$$l/k = a_\nu, \tag{3.2}$$

where a_ν denotes an eigenvalue of A.

Relation (3.2) can be found by inserting (3.1) into system (2.2). We assume that k and l are real.

If the system (2.2) is replaced by the difference scheme (2.3), the frequency l is generally changed into a different, and possibly complex frequency which we denote by l'.

Consequently, we have in case of equation (2.3) for the amplitude and velocity of the Fourier component, respectively,

$$\hat{u}(k)e^{\mathrm{Im}(l')t} \text{ and } \mathrm{Re}(l')/k.$$

The concept of a complex propagation factor T has been introduced by Leendertse [2],

$$T(x, \Delta t, \xi) = \frac{e^{i(kx-l't)}}{e^{i(kx-lt)}}.$$

We follow the propagation factor over a time interval in which the component with frequency l propagates over its wavelength. Then, for $t = -2\pi/l$,

$$T(x, \Delta t, \xi) = \exp[2\pi i\{(l'/l) - 1\}]. \tag{3.3}$$

The modulus and argument of T represent measures for the numerical damping and phase shift respectively.

Using (3.2) and (3.3), we may derive

$$|T(x, \Delta t, \xi)| = \exp[2\pi \mathrm{Im}(l')/(ka_\nu)] \tag{3.4}$$

and

$$\arg[T(x, \Delta t, \xi)] = 2\pi[\mathrm{Re}(l')/(ka_\nu) - 1]. \tag{3.5}$$

The velocity ratio Q will be given by $Q = \mathrm{Re}(l')/(ka_\nu)$. (3.6)

We substitute the component $\hat{u}(k)e^{i(kx-l't)}$ into equation (2.3) with constant coefficients; then it can be shown that

$$[G(x, \Delta t, \xi) - e^{-il'\Delta t} I]\hat{u}(k) = 0,$$

where I is the unit matrix, and G is the amplification matrix of the difference scheme again.

Thus we find a relation for l':

$$g_\nu(x, \Delta t, \xi) = e^{-il'\Delta t}; \tag{3.7}$$

here g_ν denotes an eigenvalue of G again.

Remembering the definition of a dissipative difference scheme in section 2, it is clear from (3.7), that for such a scheme we have $\mathrm{Im}(l') < 0$, for all $\xi \neq 0$. Hence dissipation goes together with damping of the Fourier components.

4. Finite-Difference Schemes

We shall use the notations:

$$u(j\Delta x, n\Delta t) \equiv u_j^n = u^n ,$$
$$Du^n = u_{j+1}^n - u_{j-1}^n , \qquad Mu^n = (u_{j+1}^n + u_{j-1}^n)/2 ,$$
$$D_1 u^n = u_{j+1}^n - u_j^n , \qquad M_1 u^n = (u_{j+1}^n + u_j^n)/2 ,$$
$$D_2 u^n = u_j^n - u_{j-1}^n , \qquad M_2 u^n = (u_j^n + u_{j-1}^n)/2 .$$

Hereafter we shall denote also the numerical solution of (2.2) by u. The following three dissipative difference schemes for the system (2.2) will be discussed.

Scheme A

$$u^{n+1} = Mu^n - \lambda/2Df^n ,$$

Scheme B

$$u^{n+1} = u^n - \lambda/2Df^n + \lambda^2/2[(M_1A^n)(D_1f^n) - (M_2A^n)(D_2f^n)] ,$$

Scheme C

$$u^{n+1} = Mu^n - \lambda/2Df^n$$
$$u^{n+2} = u^n - \lambda Df^{n+1} .$$

Scheme A is a first-order-accurate difference scheme given by Lax [5].

In [6] Lax and Wendroff introduced scheme B. This scheme has second-order accuracy.

Scheme C is the two-step Lax-Wendroff procedure found by Richtmyer [7]. If the coefficients are constant, it changes over to scheme B, though with mesh spacings $2\Delta x$ and $2\Delta t$.

The local amplification matrix G of scheme A, as derived in [8], is

$$I \cos \xi - i\lambda A \sin \xi , \tag{4.1}$$

in case of scheme B matrix G is

$$I - i\lambda A \sin \xi - \lambda^2 A^2 (1 - \cos \xi) , \tag{4.2}$$

whilst in case of scheme C matrix G is

$$I - i\lambda A \sin 2\xi - \lambda^2 A^2 (1 - \cos 2\xi) . \tag{4.3}$$

Denote λa_ν by μ; then it is clear that the eigenvalues g of the amplification matrices (4.1), (4.2) and (4.3) are, in the same order,

$$\cos \xi - i\mu \sin \xi , \tag{4.4}$$
$$1 - i\mu \sin \xi - \mu^2(1 - \cos \xi) , \tag{4.5}$$
$$1 - i\mu \sin 2\xi - \mu^2(1 - \cos 2\xi) . \tag{4.6}$$

The amplification matrices of the schemes above are all three polynomials in the matrix A, hence their eigenvectors are the same as those of A, constituting a complete set of linearly independent eigenvectors, not depending on λ and ξ. Therefore, according to the theorem of section 2, the von Neumann condition is sufficient as well as necessary for stability. It is easily established that applying this condition to the eigenvalues (4.4), (4.5) and (4.6) yields for the three schemes the well-known necessary stability condition by Courant, Friedrichs and Lewy [9]:

$$|\mu| \leqq 1 . \tag{4.7}$$

From (4.4) we obtain for the eigenvalues g_ν of matrix (4.1):

$$|g_v|^2 = 1-(1-\mu^2)\sin^2\xi\,. \tag{4.8}$$

According to the definition in section 2 we conclude that scheme A is dissipative of second order, if $|\mu|<1$.

From (4.5) we obtain in case of scheme B

$$|g_v|^2 = 1-4\mu^2(1-\mu^2)\sin^4\tfrac{1}{2}\xi\,, \tag{4.9}$$

whilst (4.6) yields for scheme C

$$|g_v|^2 = 1-4\mu^2(1-\mu^2)\sin^4\xi\,. \tag{4.10}$$

Relations (4.9) and (4.10) show that the schemes B and C are dissipative of fourth order, provided that $|\mu|<1$.

Relations (3.4) and (3.6) together with relation (3.7) and each of the expressions (4.4) through (4.6) can be combined into the following relations for

scheme A

$$|T| = (\cos^2\xi+\mu^2\sin^2\xi)^{\pi/(\mu\xi)} \tag{4.11}$$

$$Q = \arctan(\mu\tan\xi)/(\mu\xi)\,, \tag{4.12}$$

scheme B

$$|T| = [1-4\mu^2(1-\mu^2)\sin^4\tfrac{1}{2}\xi]^{\pi/(\mu\xi)} \tag{4.13}$$

$$Q = \arctan\left(\frac{\mu\sin\xi}{1-2\mu^2\sin^2\frac{1}{2}\xi}\right)\Big/(\mu\xi)\,, \tag{4.14}$$

scheme C

$$|T| = [1-4\mu^2(1-\mu^2)\sin^4\xi]^{\pi/(2\mu\xi)} \tag{4.15}$$

$$Q = \arctan\left(\frac{\mu\sin 2\xi}{1-2\mu^2\sin^2\xi}\right)\Big/(2\mu\xi)\,. \tag{4.16}$$

The phase shift is related to the velocity ratio by

$$\arg(T) = 2\pi(Q-1)\,. \tag{4.17}$$

Figures 1 through 6 show sets of curves of relations (4.11) through (4.17) for different values of μ; the wavelength is denoted by L, i.e., $L/\Delta x = 2\pi/\xi$.

In section 3 it has been argued that dissipation goes together with damping of the Fourier components. One can see from Figures 1, 3 and 5 that especially the short-wavelength components are attenuated (see also [4]).

Figures 2, 4 and 6 show clearly that the schemes A, B and C are dispersive. Again especially the short-wave components are affected.

In section 6 we shall apply scheme B to the equations of the shallow water theory while providing at once a confirmation of the results above.

5. Shallow Water Flow

The following experiments have been carried out by Cavaillé [3].

A basin with a horizontal, rectangular and smooth bottom is divided into two parts by a slide. The basin is filled with water; we denote the depths of the fluid on either side of the slide by h_0 and h_1, with $h_0>h_1$.

The slide is rapidly pulled up and after a short time interval a discontinuity in the elevation of the fluid (bore) is observed, propagating with side 1 as the front side. (Hereafter side 0 will be called the back of the bore).

In the other direction a rarefaction wave propagates, resulting in a decreasing elevation.

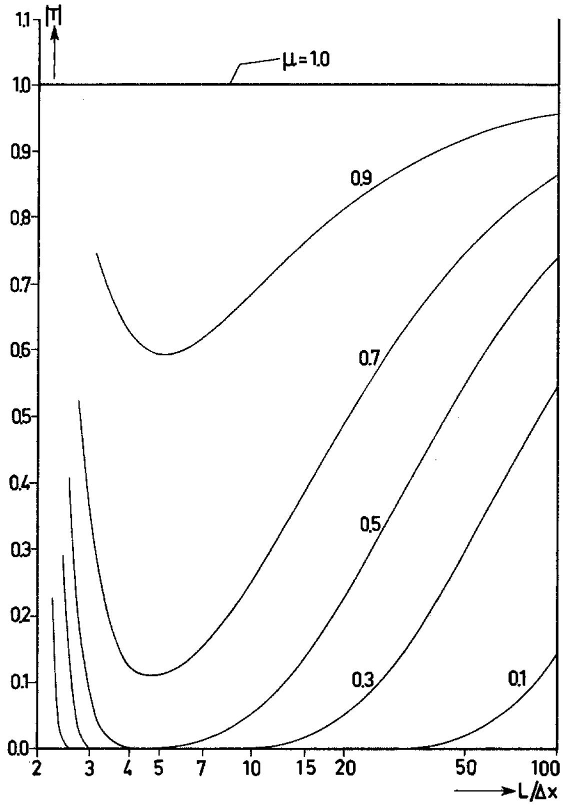

Fig.1. Scheme A: Numerical damping as given by (4.11).

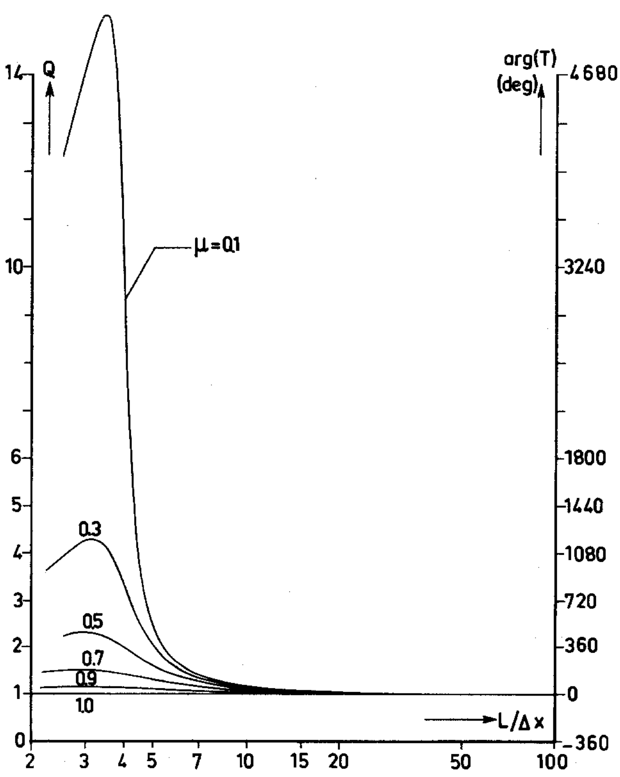

Fig. 2. Scheme A: Velocity ratio and phase shift as given by (4.12) and (4.17).

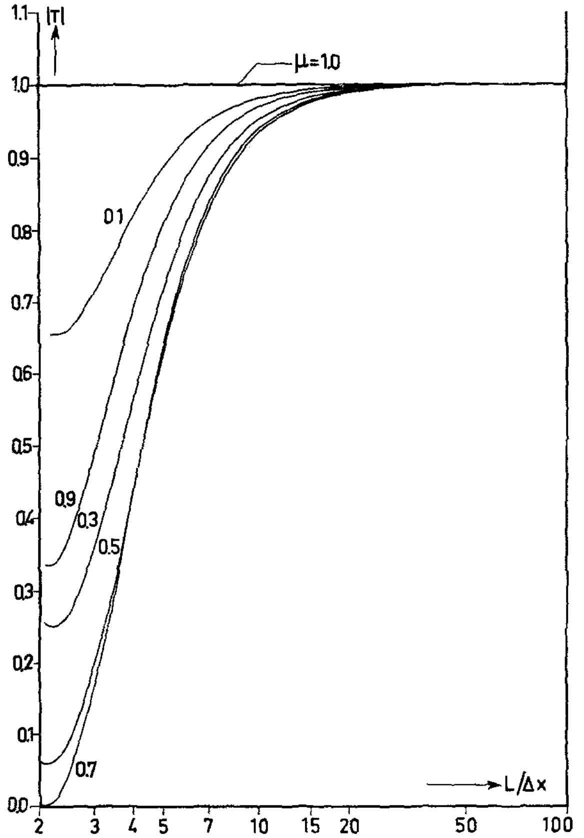

Fig. 3. Scheme B: Numerical damping as given by (4.13).

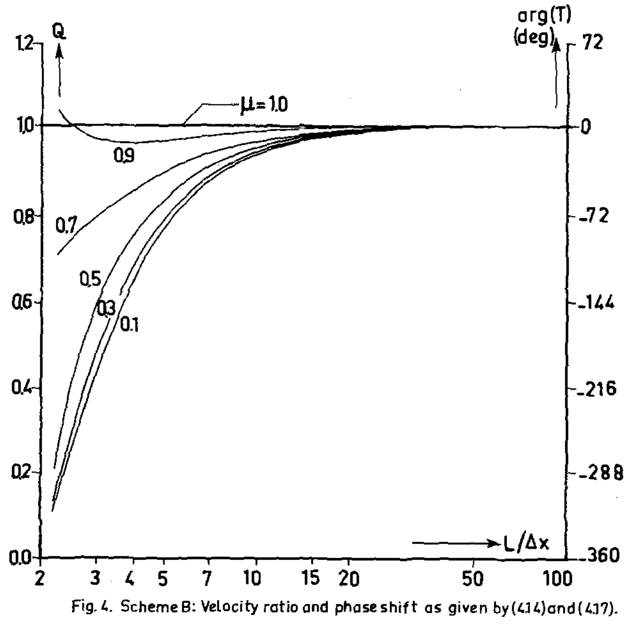

Fig. 4. Scheme B: Velocity ratio and phase shift as given by (4.14) and (4.17).

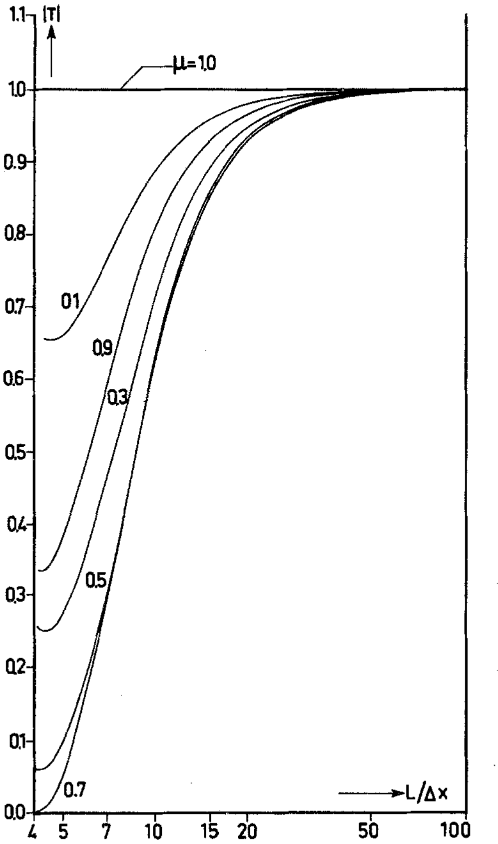

Fig. 5. Scheme C: Numerical damping as given by (4.15).

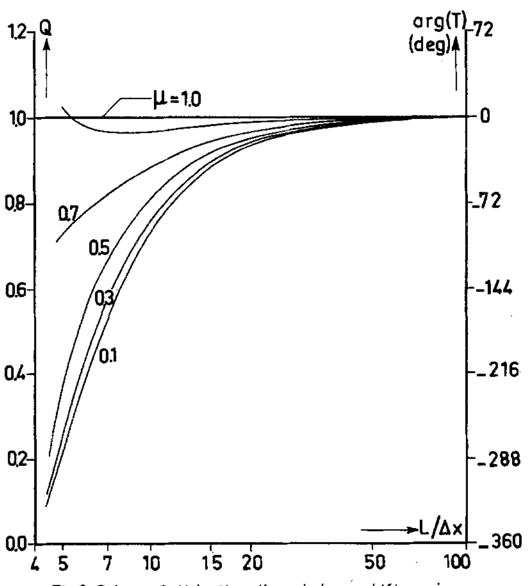

Fig. 6. Scheme C: Velocity ratio and phase shift as given by (4.16) and (4.17).

TABLE 1

depths		laboratory	numerical results					
at $t=0$		results	system (5.4)			system (5.5)		
h_0	h_1	q	q	h_2	v_2	q	h_2	v_2
1	0.696	0.96	0.96	0.84	0.17	0.96	0.84	0.17
1	0.348	0.93	0.91	0.63	0.41	0.94	0.63	0.42
1	0.174	0.90	0.87	0.51	0.57	0.96	0.48	0.61
1	0.043	0.98	0.84	0.39	0.75	1.07	0.29	0.92

Dimensionless values of the velocity of propagation of the bore, denoted q, measured for different ratios of h_0 and h_1, have been listed in Table 1. For dimensionless variables see below in this section.

We shall compare the experimental results by Cavaillé with solutions of the shallow water theory (see Stoker [1]), determined by the equation of conservation of mass

$$\frac{\partial h}{\partial t} + \frac{\partial}{\partial x}(hv) = 0\,, \tag{5.1}$$

and the equation of motion in the x-direction

$$\frac{\partial v}{\partial t} + v\frac{\partial v}{\partial x} + g\frac{\partial h}{\partial x} = 0\,. \tag{5.2}$$

The space and time coordinates are denoted by x and t; h denotes the depth of the fluid, v the velocity in the (horizontal) x-direction and g the acceleration due to gravity.

Multiplying equation (5.1) by v and (5.2) by h, and adding the equations together, yields the equation of conservation of momentum

$$\frac{\partial}{\partial t}(hv) + \frac{\partial}{\partial x}(hv^2) + gh\frac{\partial h}{\partial x} = 0\,. \tag{5.3}$$

This equation can also be derived by integration of (5.2) with respect to the vertical space coordinate and making use of (5.1).

By combining equations (5.1) and (5.2) we also get

$$\frac{\partial}{\partial t}\left[\tfrac{1}{2}(hv^2+gh^2)\right] + \frac{\partial}{\partial x}\left[\tfrac{1}{2}v(hv^2+gh^2)\right] + \tfrac{1}{2}g\frac{\partial}{\partial x}(h^2v) = 0\,,$$

expressing the conservation of energy, i.e. the sum of kinetic and potential energy.

We introduce dimensionless variables:

$$\begin{aligned} &\bar{x} = x/h_0 && \bar{v} = v/\sqrt{gh_0} \\ &\bar{t} = t\sqrt{g/h_0} && \bar{g} = g/g = 1\;; \\ &\bar{h} = h/h_0 && \end{aligned}$$

h_0 denotes again the depth on the upstream side before the slide is pulled up.

Using the dimensionless variables and leaving out the bars, we may write the system which consists of the equations (5.1) and (5.2) in the notation (2.1)

$$\frac{\partial}{\partial t}\begin{pmatrix} h \\ v \end{pmatrix} + \frac{\partial}{\partial x}\begin{pmatrix} hv \\ \tfrac{1}{2}v^2 + h \end{pmatrix} = 0\,. \tag{5.4}$$

Similarly equations (5.1) and (5.3) yield the system

$$\frac{\partial}{\partial t}\begin{pmatrix} h \\ \varphi \end{pmatrix} + \frac{\partial}{\partial x}\begin{pmatrix} \varphi \\ \varphi^2/h + \tfrac{1}{2}h^2 \end{pmatrix} = 0\;;\ \varphi \text{ is called the discharge, } \varphi = hv. \tag{5.5}$$

It will be clear that the systems (5.4) and (5.5) are equivalent in the case of a continuous solution. Consequently, the eigenvalues of the matrix A are for both systems

$$a_v = v \pm \sqrt{h}\,, \tag{5.6}$$

representing the speeds of progressive and retrogressive waves.

In the case of continuous solutions one would prefer system (5.4) for calculations; then, it follows from above that momentum and energy are conserved.

We shall show that in the case of a discontinuous solution the two systems are not equivalent at all.

6. Numerical Results

The calculations described below have been carried out with difference scheme B.

Suppose the slide in the basin (see section 5) is pulled up at $t=0$; thus, we take as initial conditions $v\equiv 0$, $h_0=1$, and, for example, $h_1=0.5$.

Figure 7 shows a computed bore extended over about three intervals Δx. In section 4 we

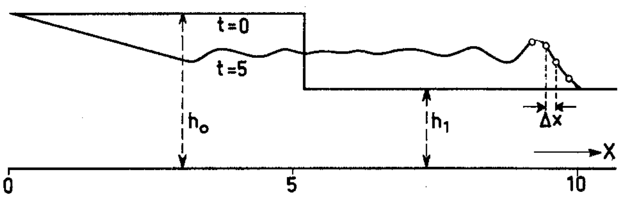

Fig. 7. Initial depths and bore computed by applying scheme B to system (5.5); $\Delta x=0.2$, $\Delta t=0.04$.

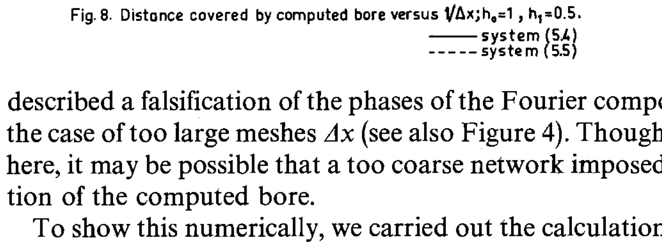

Fig. 8. Distance covered by computed bore versus $1/\Delta x$; $h_0=1$, $h_1=0.5$.
—— system (5.4)
----- system (5.5)

described a falsification of the phases of the Fourier components for the numerical solution in the case of too large meshes Δx (see also Figure 4). Though a linear analysis is not appropriate here, it may be possible that a too coarse network imposed on the x, t-space, causes a retardation of the computed bore.

To show this numerically, we carried out the calculations with different values of Δx, whilst Δt is such that the ratio $\lambda = \Delta t/\Delta x$ keeps the constant value 0.2 in order to satisfy the stability condition

$$\lambda(|v| + \sqrt{h}) \leqq 1\,,$$

which is obtained from relations (4.7) and (5.6).

The distance covered by the computed before versus $1/\Delta x$ is shown in Figure 8 for the time intervals $0 \leqq t \leqq 5$ and $5 \leqq t \leqq 10$.

The x-value for which the depth of the fluid equals the average value of the depths on both sides of the bore will also represent the position of the bore; it is determined by linear interpolation.

Figure 8 shows that the distance covered during the time interval $0 \leqq t \leqq 5$ keeps increasing for the considered values of Δx, whilst the distance covered during the time interval $5 \leqq t \leqq 10$ is approximately constant for $\Delta x < 0.25$.

This can be explained by the following argument.

At the instant $t=0$ a genuine discontinuity is present. The computed bore presents itself not just as a discontinuity, however, but as a strong gradient of depth and velocity of the fluid (see also Figure 7). Thus, it may be expected that the Fourier series for the computed bore contains less short-wave components than the Fourier series for the discontinuity at $t = 0$, and from section 4 it is clear that the retardation of the bore occurs especially at the start of the computation.

In the case of a stronger bore we obtained the same results: the graphs in Figure 9 show about

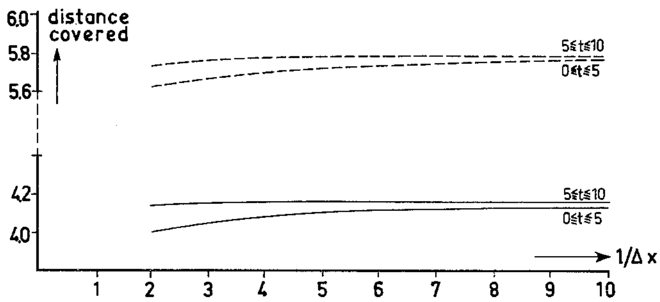

Fig. 9. Similar to figure 8, except that $h_1 = 0.02$.

the same feature as those in Figure 8, though in the case of system (5.5) the bore velocity is significantly larger than in the case of system (5.4).

We compared our numerical results with the experimental results obtained by Cavaillé. To minimize the retardation described above, we used

$$\Delta x = 0.1 \text{ and } \Delta t = 0.02 \text{ for } 0 < t < 5\,, \text{ and } \Delta x = 0.2 \text{ and } \Delta t = 0.04 \text{ for } t \geqq 5\,.$$

Values of the computed bore velocity q, together with values of depth and velocity of the fluid behind the bore, h_2 and v_2, have been listed in Table 1.

In addition, analytic calculations were carried out using the generalized Rankine-Hugoniot relations (see the next section) applied to the systems (5.4) and (5.5). The results agreed well with the numerical results (see [8]).

7. A Local Instability

In the case of system (5.5) and for $h_1 = 0.174$ and $h_1 = 0.043$ an instability was observed. This occurred at the position of the jump, and directly after $t=0$.

Figure 10 shows the depth h as a function of x for various numbers of time-steps. For $t > 0.8$ the depth becomes even negative locally, whilst the velocity increases more and more.

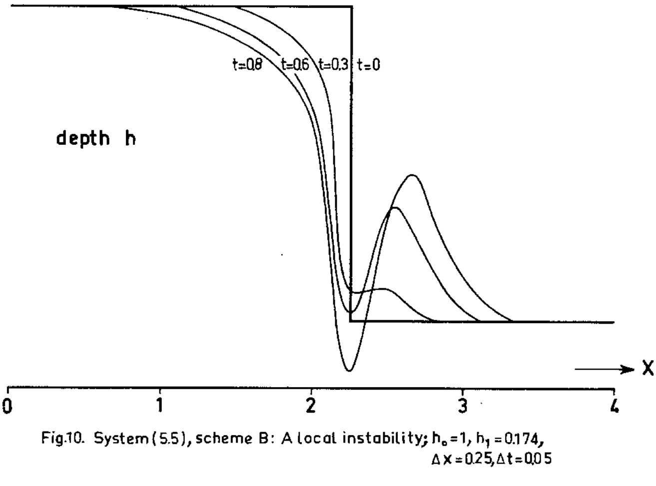

Fig. 10. System (5.5), scheme B: A local instability; $h_0 = 1$, $h_1 = 0.174$, $\Delta x = 0.25$, $\Delta t = 0.05$

By using different mesh sizes, we may conclude that the instability is independent of the fineness of the net and also of the ratio $\lambda = \Delta t/\Delta x$. This local and nonlinear instability has been found by Burstein [10] during numerical calculation of supersonic flow in three independent variables. Our argument, as does Burstein's, is based on a local and partial absence of numerical damping.

For the eigenvalue $v-\sqrt{h}$ of the matrix A we have on the front side of the bore

$$v-\sqrt{h} = -\sqrt{h} < 0 .$$

The generalized Rankine-Hugoniot relation (see also Lax [11]) for equation (2.1) takes the form

$$q[u] = [f] , \tag{7.1}$$

where [ ] denotes the jump across the discontinuity, and q is again the velocity of propagation of the discontinuity.

We apply relation (7.1) to system (5.4) and, taking into account that the velocity v on the front-side of the bore equals zero, it can be shown that behind the bore we have

$$v_2 = (h_2 - h_1)\sqrt{\frac{2}{h_1+h_2}} ,$$

and thus also

$$v-\sqrt{h} = (h_2-h_1)\sqrt{\frac{2}{h_1+h_2}} - \sqrt{h_2} = \frac{2h_1^2 - 5h_1h_2 + h_2^2}{N_1} ,$$

where N_1 is definite-positive.

The right member of this relation, and thereby the eigenvalue $v-\sqrt{h}$ is positive for $h_2/h_1 >$ 4.56. (In fact also for $h_2/h_1 < 0.44$, but this is not taken into consideration here).

Similarly, applying relation (7.1) to system (5.5) yields with $v_1 = 0$:

$$v_2 = (h_2 - h_1)\sqrt{\frac{h_1+h_2}{2h_1h_2}} ,$$

and behind the bore,

$$v-\sqrt{h} = (h_2-h_1)\sqrt{\frac{h_1+h_2}{2h_1h_2}} - \sqrt{h_2} = \frac{h_1^3 - h_1^2h_2 - 3h_1h_2^2 + h_2^3}{N_2} ,$$

where N_2 is definite-positive.

Therefore, in this case, the eigenvalue $v-\sqrt{h}$ is positive for $h_2/h_1 > 3.21$. It follows that for both systems (5.4) and (5.5), and for a strong jump, i.e., a large ratio h_2/h_1, the sign of one of the eigenvalues of the matrix A changes across the jump. We may expect that this eigenvalue will be zero somewhere in the region of the computed bore, and considering relation (4.9) leads to the conclusion that here the difference scheme is not dissipative: no damping of the short-wave components is performed by the eigenvalue $v-\sqrt{h}$.

Hence dissipation is absent just where it is necessary for a stable solution. The remedy to prevent the instability in our calculations is to give, as initial condition, the jump in h over two intervals Δx, instead of over one interval Δx (see Figure 11).

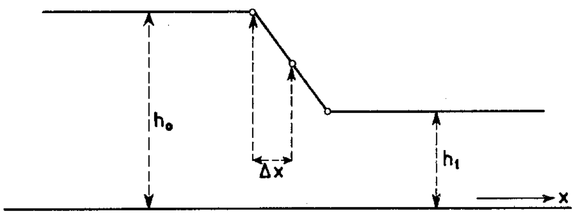

Fig.11. Initial conditions to prevent nonlinear instability.

8. Conclusions

The equivalence of the systems (5.4) and (5.5) in the case of smooth solutions has been mentioned in section 5. From the results in section 6 it follows, however, that the discontinuous solutions of the two systems are different.

Lax [11] pointed out that in hydrodynamics the system consisting of the equations of conservation of mass, momentum, and energy on one hand, and the system of the equations of conservation of mass, momentum, and entropy on the other hand, are equivalent in case of smooth solutions, but are not equivalent in the discontinuous case.

We consider in the shallow fluid flow a column at the position of the jump, as shown in Figure 12.

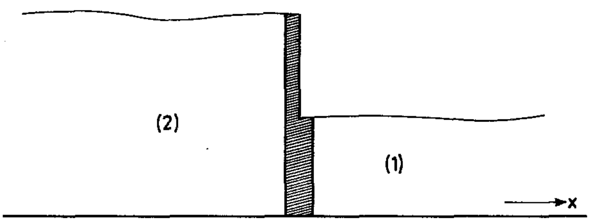

Fig.12. Cross-section view with column at the position of the jump.

For this column the conservation of momentum is expressed by

$$h_1(v_1-q)v_1-h_2(v_2-q)v_2+\tfrac{1}{2}gh_1^2-\tfrac{1}{2}gh_2^2=0\,. \tag{8.1}$$

The first two terms on the left side of (8.1) represent the change in momentum of the column per unit time, whilst the force acting on the end sections of the column is represented by the last two terms. Equation (8.1) can also be derived by applying the generalized Rankine-Hugoniot relation (7.1) to equation (5.3).

On the contrary, application of (7.1) to equation (5.2) yields a relation which cannot be interpreted as a conservation law.

As it can also be established that the Rankine-Hugoniot relation of equation (5.1) expresses the conservation of mass across the jump, we may conclude that the conservation of mass and momentum is exactly satisfied by the jump relations of system (5.5).

Remembering the theory of weak solutions (see Lax [11]), it can be said that the physically correct jump relations belong to the piecewise continuous weak solutions of (5.5).

Therefore we prefer (5.5) for the calculation of a discontinuous solution in shallow fluid theory.

In [12] the problem of calculating a bore from the shallow water equations has been solved by using the von Neumann-Richtmyer method (see [4]); here however, use has been made of system (5.4), which is not acceptable from the physical point of view.

The solutions of system (5.5) are, as can be seen in Table 1, not very satisfying, especially if the jump grows stronger. This can be explained by the argument that the shallow water equations are not appropriate to this problem: they have been derived on the assumption that the pressure is given as in hydrostatics (see Stoker [1]). This assumption, however, is completely incorrect if a discontinuity is present in the flow.

Nevertheless, as Table 1 shows, a weak bore is governed rather well by the shallow water equations.

Acknowledgement

The author wishes to express his gratitude to Prof. dr. E. van Spiegel. His helpful comments and advice made this work possible.

REFERENCES

[1] J. J. Stoker; *Water waves*, Interscience Publishers, New York, 1957.
[2] J. J. Leendertse; *Aspects of a computational model for long-period water-wave propagation*, Doctoral Thesis, Delft University of Technology, 1967.
[3] J. Cavaillé; Contribution à l'étude de l'écoulement variable accompagnant la vidange brusque d'une retenue, *Publ. Ministère de l'Air*, No. 410, 1965.
[4] R. D. Richtmyer and K. W. Morton; *Difference methods for initial-value problems*, 2nd edition, Interscience Publishers, New York, 1967.
[5] P. D. Lax; Weak solutions of nonlinear hyperbolic equations and their numerical computation, *Comm. Pure Appl. Math.*, Vol. 7, pp. 159–193, 1954.
[6] P. D. Lax and B. Wendroff; Systems of conservation laws, *Comm. Pure Appl. Math.*, Vol. 13, pp. 217–237, 1960.
[7] R. D. Richtmyer; A survey of difference methods for non-steady fluid dynamics, *N.C.A.R. Tech. Note* 63–2, 1963.
[8] A. C. Vliegenthart; Berekeningen van discontinuïteiten in ondiep water, *Report NA*-4, *Math. Inst.*, Delft University of Technology, 1968.
[9] R. Courant, K. O. Friedrichs and H. Lewy; On the partial difference equations of math. physics, *N.Y.U. Courant Inst. Math. Sci. Res. Dept., N.Y.O.*-7689, 1956.
[10] S. Z. Burstein; Finite-difference calculations for hydrodynamic flows containing discontinuities, *J. Comp. Physics*, Vol. 1, pp. 198–222, 1967.
[11] P. D. Lax; Hyperbolic systems of conservation laws, *Comm. Pure Appl. Math.*, Vol. 10, pp. 537–566, 1957.
[12] A. Preissmann and J. A. Cunge; Calcul du mascaret sur machine électronique, *La Houille Blanche*, No. 5, 1961.

Journal of Engineering Math., Vol. 3 (1969) 81–94